International Journal of Heat and Fluid Flow 106 (2024) 109316

Contents lists available at ScienceDirect

International Journal of Heat and Fluid Flow

journal homepage: www.elsevier.com/locate/ijhff

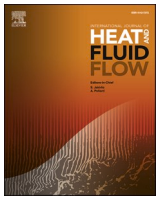

Performance of boilers equipped with vapor-pump (BEVP) system equipped with a novel air-flue gas total heat exchanger

Jing Hua [a], Jingyi Wang [b], Tingting Zhu [c,*]

[a] College of Civil Engineering, Taiyuan University of Technology, Taiyuan, Shanxi, China
[b] School of Science, Harbin Institute of Technology, Shenzhen, Guangdong, China
[c] University of Twente, Faculty of Engineering Technology, 7522 NB Enschede, The Netherlands

ARTICLE INFO

Keywords:
Gas nonlinearity
Total heat recovery
Flue gas
Heat recovery efficiency

ABSTRACT

Because of high humidity and nonlinearity of flue gas, waste heat from flue gas is hard to recovery. Boilers equipped with vapor-pump system is developed to solve the problem caused by high humidity. In this system, double spray towers subsystem is equipped to realize total heat waste heat recovery. However, caused by nonlinearity, limited waste heat recovery efficiency is just 83 % (1 segment) and 93 % (2 segment). Further, based on boilers equipped with vapor-pump (BEVP) system, enthalpy wheel system is developed to solve the problem caused by nonlinearity. However, enthalpy wheel system cannot solve the problem completely. In this article, a novel air-flue gas total heat exchanger is put forward to achieve full waste heat recovery. In this system, waste heat recovery efficiency limit is up to 100 %. Then, the limit condition of total heat transfer process is discussed. Performance of the total heat exchanger is discussed and compared to double spray towers system and enthalpy wheel system. As the result, considering heat transfer temperature difference, the total heat exchanger total heat transfer efficiency of the total heat exchanger is 7 % higher than 2-segment BEVP system and 10 % higher than enthalpy wheel system.

1. Introduction

1.1. Background

Waste heat recovery is an effective method to improve energy efficiency, alleviate energy crisis and promote carbon neutrality in China. Natural gas is widely used as clean energy source to reduce environmental pollution, and biomass gas is an important fuel to achieve carbon neutrality. So that, researchers have dedicated to improving gas boiler efficiency for many years. Waste heat recovery from flue gas discharged from gas boilers plays an important role in gas boiler efficiency improvement.

Currently, there are three main methods of flue gas waste heat recovery: (1) waste heat is recovered directly by fresh air or return water (Ma et al., 2021; Han et al., 2021; Mohammadaliha et al., 2022; Min et al., 2021; Zhang et al., 2020; Wei et al., 2022; Xiao et al., 2021; Yang and Yuan, 2022; Xiao et al., 2019) (Fig. 1 (a)); (2) waste heat is recovered by return water via absorption/electric heat pump (Zhang et al., 2021; Zhang et al., 2020; Zhang et al., 2022; Yang et al., 2020; Yu et al., 2021; Cui et al., 2020; El-Shafie et al., 2021; Wang et al., 2020; Jiang et al., 2021) (Fig. 2); (3) waste heat is recovered through total heat exchange between fresh air and flue gas (Wang et al., 2020; Wang et al., 2019; Men et al., 2019; Men et al., 2021; Men et al., 2022).

With respects to the first method, because fresh air humidity is far less than flue gas, heat recovery efficiency is very low (Ma et al., 2021; Han et al., 2021; Mohammadaliha et al., 2022; Min et al., 2021; Zhang et al., 2020; Wei et al., 2022; Xiao et al., 2021). Dew point of gas fired boiler flue gas is about 45 °C. In the total heat content of flue gas, the ratio of latent heat is around 40 %. In Fig. 1(b), as showed in enthalpy-humidity chart, when air is heated from 0 °C to 45 °C, saturated air can be cooled from 45 °C to 40.2 °C. Because of thermophysical property of flue gas is very close to fresh air, so that, as shown in Fig. 1(c), when fresh air is heated from 0 °C to 45 °C, flue gas is cooled from 45 °C to 40 °C. Therefore, heat recovery efficiency is very low. On the other hand, when return water of district heating (DH) system is used as cold source in a recovery system, because return water temperature is only as low as around 40 °C, as shown in Fig. 1(c), heat recovery efficiency is also very low. If the temperature of cooling water decreases, the efficiency can increase (Ma et al., 2021; Wei et al., 2022). Moreover, transport membrane condenser also can be used in the system (Xiao et al., 2021; Yang and Yuan, 2022; Xiao et al., 2019), but it cannot

* Corresponding author.
E-mail address: t.zhu@utwente.nl (T. Zhu).

https://doi.org/10.1016/j.ijheatfluidflow.2024.109316
Received 24 October 2023; Received in revised form 13 January 2024; Accepted 12 February 2024
Available online 16 February 2024

Nomenclature

C/Cp	specific heat
F	area
H/h	enthalpy
K	heat transfer coefficient
m	quality
Q	heat flow
r	latent heat of water vaporization
T	temperature
x	length

Greeks

η	efficiency

Abbreviation

BEVP	boilers equipped with vapor-pump
DT	double spray towers
EW	enthalpy wheel
NTHE	novel total heat exchanger

Subscript

air	fresh air
con	heat conduction
dry	dry air/flue gas
gas	flue gas
m	mean
out	outlet
sup	supply
T	temperature
t	total
vapor	vapor in fresh air or flue gas
water	supply/condensed water

increase efficiency greatly.

With respects to the second method, due to the participation of heat pumps driven by high temperature heat source or electric power, flue gas can be cooled down below 20 °C (Yu et al., 2021; Cui et al., 2020; Jiang et al., 2021). These methods can guarantee flue gas waste heat recovery efficiency but cost of these systems is very high.

With respects to the third method, to make full use of low temperature cold source from fresh air, air humidification is considered in the heat recovery system, so that, with the increase of fresh air enthalpy, heat recovery capacity of fresh air is increased. Under this idea, if sufficient heat transfer is possible, flue gas temperature can be cooled down to fresh air temperature, and this heat transfer process is just like total heat transfer process. In order to humidify fresh air, spray tower is used in BEVP system, and then, this BEVP system is analyzed and optimized by Wang et al. (2020, 2019), see Fig. 3.

1.2. Limitation of the BEVP system

In a BEVP system, total heat exchange is achieved through spray water, so that both flue gas and fresh air is saturated in the heat transfer process. Both fresh air and flue gas have enthalpy nonlinear characteristics. The enthalpy of fresh air and flue gas change nonlinearly with temperature, while spray water enthalpy changes linearly with temperature. Therefore, if water is used as intermediary fluid for total heat exchange, there will be a heat exchange limit in the Subsystem II. Main component of Subsystem II is two spray towers, so Subsystem II is abbreviated by DT (double spray towers) system. The enthalpy variation of fresh air, flue gas and spray water cannot match appropriately, shown in Fig. 4. Thus, limited waste heat recovery efficiency is just 83 %. In order to break through this limit, multi-stage heat and mass exchange process is put forward. If there are infinite heat and mass transfer stages, the total heat recovery efficiency of the Subsystem II can achieve 100 %.

Another method to solve the problem caused by gas nonlinearity is proposed by Men et al. (2019, 2021, 2022). An enthalpy wheel (EW) system is considered to replace Subsystem II in BEVP system (Men et al., 2019, 2021, 2022), see Fig. 5. In this system, Intermediate flow is cancelled. Heat and humidity are transferred by wet wall in EW. The EW device can be regarded as a combination of infinite sets of spray towers pairs, see Fig. 6, serving as an infinite-stage heat and mass exchange process. However, the difference of the two systems proposed by Wang and Men is that, the heat and mass transfer in Subsystem II is a counter flow process, while EW system is similar to a cross flow process. As a result, total heat recovery rate of EW system cannot achieve 100 %.

1.3. The aim of paper

To solve the problem caused by gas nonlinearity, this paper proposed a novel total heat exchanger. In this system, waste heat recovery efficiency limit is up to 100 %. In this paper, the limit condition of total heat transfer process is put forward. Performance of the novel total heat exchanger is discussed by numerical simulation and compared to DT system and EW system.

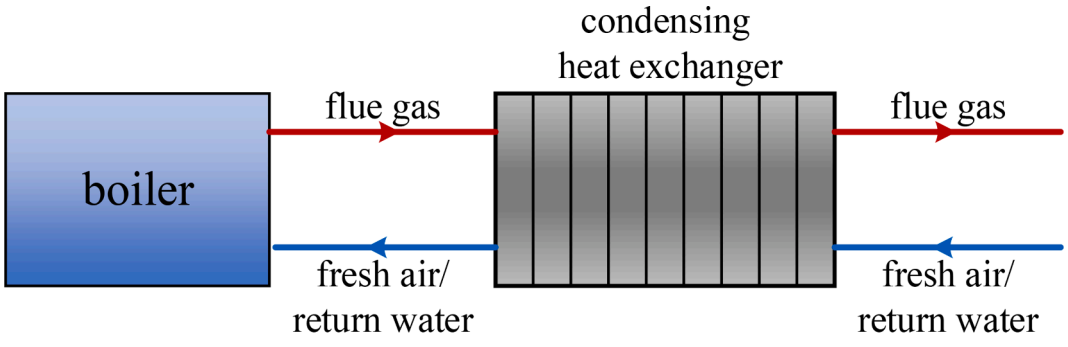

(a) The scheme of direct heat recovery system

Fig. 1. Heat is recovered by fresh air and return water directly.

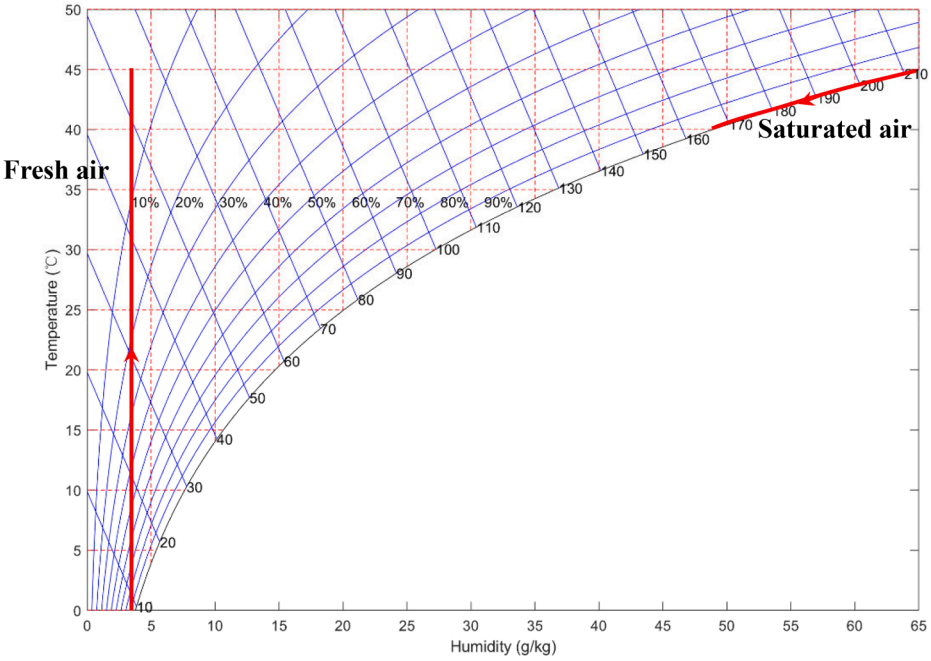

(b) Heat transfer between fresh air and saturated air

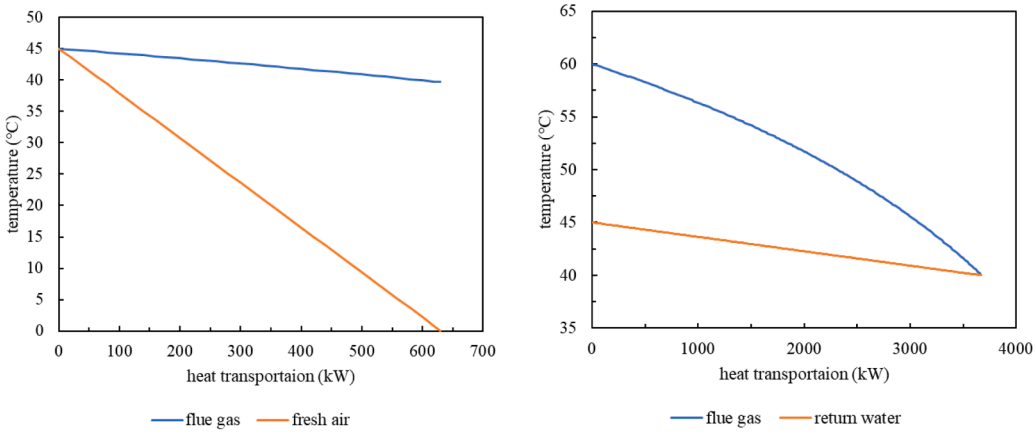

Heat recovered by fresh air Heat recovered by return water

(c) T-Q chart of direct heat recovery system: the outlet temperature of flue gas is very high (compared to 0℃)

Fig. 1. (*continued*).

2. Heat and mass transfer characteristics of the new total heat exchanger

2.1. Structure of the new total heat exchanger

The novel total heat exchanger (NTHE) replaces DT system (Subsystem II) in BEVP system, see Fig. 7. In this system, flue gas is cooled by cooling water at first, and the flue gas at the outlet of the condensing heat exchanger is saturated flue gas. In the condensing heat exchanger, a part of vapor is condensed. The condensing heat exchanger is equipped with a water catchment plate and a water trap through which the drain water is discharged from the heat exchanger. The drain water is acidic and needs to be neutralized before it is drained away. Then saturated flue gas is cooled by fresh air in NTHE. On the other hand, fresh air is heated and humidified by saturated flue gas in NTHE.

Structure of NTHE is showed in Fig. 8, the structure is based on plate heat exchanger, and there are two water films on the surface of heat exchange plate. In NTHE's heat transfer channel (see Fig. 8(b)), vapor in flue gas is condensed on the surface of heat exchange plate, the condensed water film is formed. In fresh air channel, drain water is collected and supplied to the surface of heat exchange plate. To distribute the fresh air and flue gas evenly in each channel, the heat exchanger is equipped with plenum chambers and infusion chambers. The bottom of the heat exchanger is equipped with a water catchment

plate and a water trap, and a water pump is used to pump the water to the top of the heat exchanger. And a water distributor at the top of the heat exchanger feeds water into the flow channel.

2.2. Heat and mass exchange theory in a NTHE

As shown in Fig. 9, in flue gas channel, vapor in flue gas is condensed on heat transfer wall, and latent heat is converted into sensible heat, and sensible heat of flue gas is transferred to condensed water film by heat convection. Then sensible heat is conducted to the air channel by heat exchange plant. In fresh air channel, sensible heat is transfer to supply water film, then sensible heat is converted into latent heat by water film evaporation, and the rest sensible heat is transferred to fresh air by heat convection. In flue gas channel, vapor is condensed and drained out. Then drained water is supplied to fresh air channel. With the help of supply water film, condensed water film and drained water reuse, total heat transfer is achieved.

In a NTHE, drain water takes away heat from flue gas channel, and supply water brings heat into fresh air channel, so that heat balance analysis of the system at micro level is needed. As illustrated in Fig. 9, heat transfer can be divided in five parts: fresh air, supply water film, heat exchange plate, condensed water film and flue gas.

In flue gas channel, heat balance is described by Eq. (1),

$$\frac{dh_{gas}}{dx} = \left(C_{p,gas,dry}m_{gas,dry} + C_{p,vapor,gas}m_{vapor,gas}\right)\frac{dT_{gas}}{dx} + r\frac{dm_{vapor,gas}}{dx} \tag{1}$$

In condensed water film, heat balance is described by Eq. (2)

$$C_{water}T_{gas}\frac{dm_{vapor,gas}}{dx} = \frac{dh_{gas}}{dx} - Q_{con} \tag{2}$$

In supply water film, heat balance is described by Eq. (3)

$$C_{water}\left(\frac{dm_{vapor,gas}}{dx} - \frac{dm_{vapor,air}}{dx}\right)T_{water,sup,out} - C_{water}T_{gas}\frac{dm_{vapor,gas}}{dx} = Q_{con} - \frac{dh_{air}}{dx} \tag{3}$$

In fresh air channel, heat balance is described by Eq. (4),

$$\frac{dh_{air}}{dx} = \left(C_{p,air,dry}m_{air,dry} + C_{p,vapor,air}m_{vapor,air}\right)\frac{dT_{air}}{dx} + r\frac{dm_{vapor,air}}{dx} \tag{4}$$

Considering the heat exchange temperature difference is small.

$$\frac{dm_{vapor,gas}}{dx} - \frac{dm_{vapor,air}}{dx} \ll \frac{dm_{vapor,gas}}{dx} \tag{5}$$

In extreme case, heat exchange temperature difference is zero.

$$\frac{dm_{vapor,gas}}{dx} - \frac{dm_{vapor,air}}{dx} = 0 \tag{6}$$

Simplify and approximate Eq. (3) based on Eq. (5) and Eq. (6), Eq. (3) can be described as

$$-C_{water}T_{gas}\frac{dm_{vapor,gas}}{dx} = Q_{con} - \frac{dh_{air}}{dx} \tag{7}$$

Combine Eq. (2) and Eq. (7), we can get Eq. (8) and Eq. (9)

$$\frac{dh_{gas}}{dx} - Q_{con} = C_{water}T_{gas}\frac{dm_{vapor,gas}}{dx} = -\left(Q_{con} - \frac{dh_{air}}{dx}\right) \tag{8}$$

$$\frac{dh_{gas}}{dx} = \frac{dh_{air}}{dx} \tag{9}$$

Eq. (9) demonstrates that total heat exchange is achieved by NTHE. According to Eq. (9), in the infinitesimal heat transfer channel, enthalpy change of flue gas and fresh air is the same. To achieve heat transfer, in each infinitesimal heat transfer channel, flue gas temperature should slightly higher than fresh air temperature; and to keep temperature difference, flue gas and fresh air temperature drop in each infinitesimal heat transfer channel should be the same. In this condition, total heat exchange between fresh air and flue gas can be achieved.

3. Simulation model of the new total heat exchanger

3.1. Physical model

The physical model of the NTHE is shown in Fig. 10. Considering the

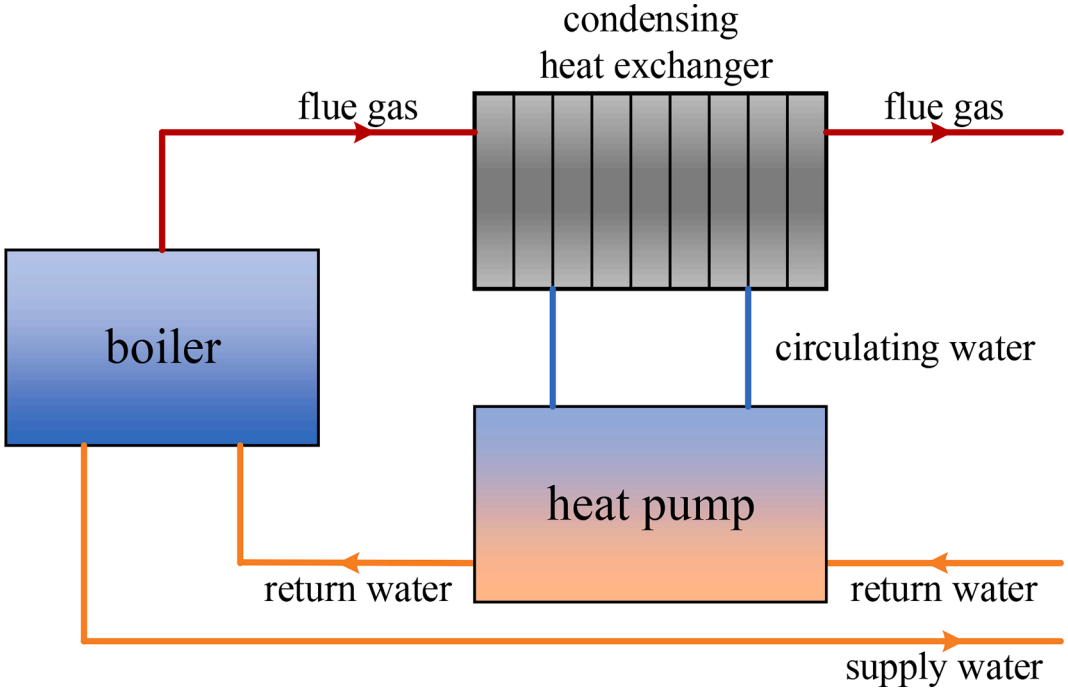

Fig. 2. Heat is recovered by return water via absorption/electric heat pump.

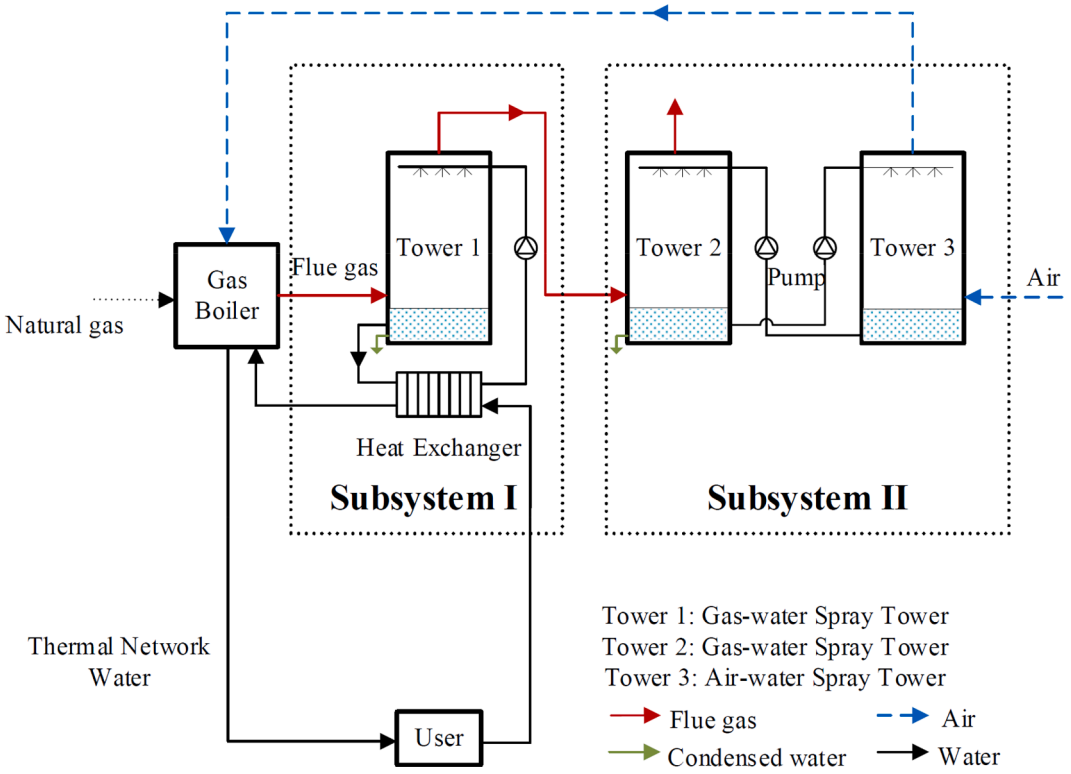

Fig. 3. The scheme of boilers equipped with vapor-pump (BEVP) system (Wang et al., 2020).

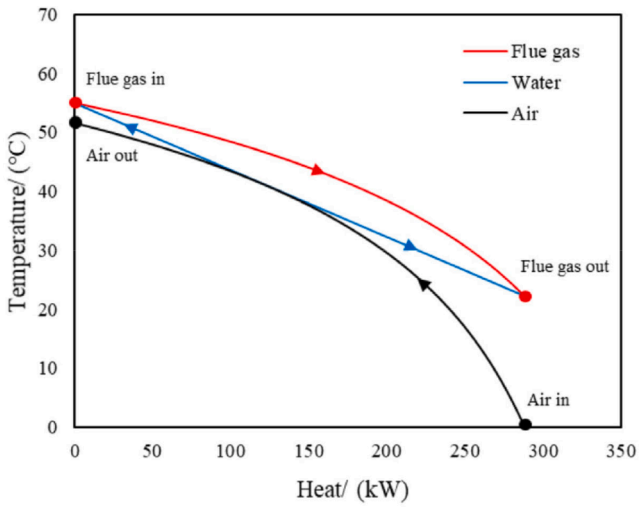

Fig. 4. Ultimate heat exchange process in subsystem ii on T-Q chart (Wang et al., 2020).

symmetry, the model includes half of the flue gas channel, half of the air channel, and the spray water film of the air preheater. Since the distance between channels is much smaller than the plate length and width, and the distribution of velocity and temperature in this direction has little effect on the performance of the air preheater, a two-dimensional model is selected to simulate the model in the x-y plane, and the heat and mass transfer in the z-direction is represented by a heat source term and a moisture source term.

3.2. Mathematical model

Referring to the dimensions of other plate heat exchangers (Wang et al., 2020, 2019; Rydstrand et al., 2004), a flat plate is selected for the heat exchanger, and a two-dimensional model is established.

The following assumptions are made for the model:

(1) Neglect the heat exchange between the heat exchanger and the external environment.
(2) Neglect the thermal resistance between the condensation water film of the flue gas and the heat exchange plate.
(3) The heat and mass transfer process are steady state.
(4) The gas is an incompressible ideal gas.
(5) The wet surface is sufficiently wetted.
(6) Neglect the influence of gravity factors.

The supply and condensing water film thickness increases from the top to the bottom. However, considering that the water film is very thin, the effect of thickness is very small, so for the sake of simplicity, water film thickness is assumed constant.

To Simplify heat transfer of the flue gas, constant pressure specific heat capacity of the gas is calculated using the enthalpy difference method based on the saturated flue gas enthalpy:

$$C_{p,g} = \frac{\Delta H_g}{\Delta t_g} \tag{10}$$

In the equation, ΔH_g represents the enthalpy difference of the gas, in $kJ{\cdot}kg^{-1}$; $C_{p,g}$ represents the constant pressure specific heat capacity of the gas, in $kJ{\cdot}(kg{\cdot}K)^{-1}$; Δt_g represents the temperature difference of the gas, in °C.

3.3. Control equations

Continuity equation:

$$\rho \nabla \boldsymbol{u} = 0 \tag{11}$$

Where ρ is the density, in $kg{\cdot}m^{-3}$; $\boldsymbol{u}$ is the velocity vector, in m/s.

Momentum equation:

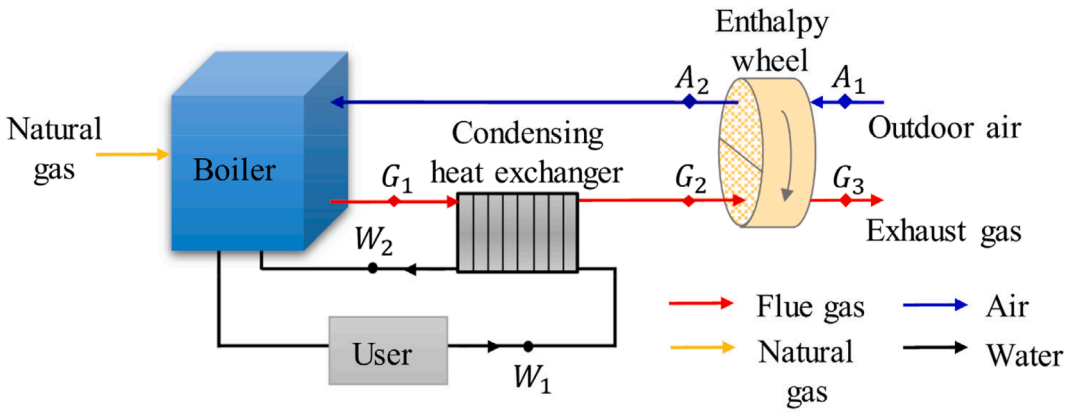

Fig. 5. The scheme of boilers equipped with enthalpy wheel (EW) system (Men et al., 2019).

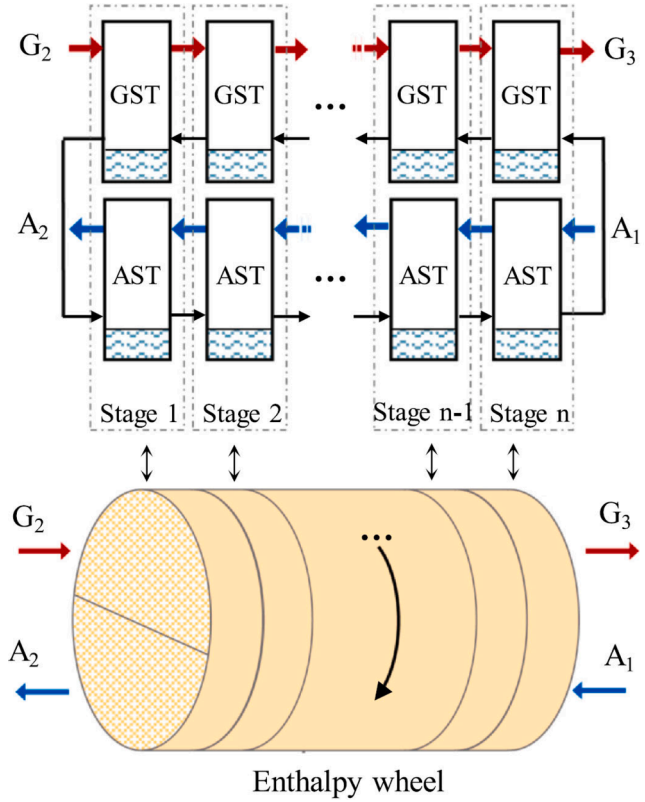

Fig. 6. The EW device can be regard as a combination of infinite sets of double spray towers (Men et al., 2022).

$$\rho(\boldsymbol{u}\bullet\nabla)\boldsymbol{u}=\nabla\bullet\left[-p+\mu\left(\nabla\boldsymbol{u}+(\nabla\boldsymbol{u})^{T}\right)\right] \tag{12}$$

Where p is the pressure, in Pa; μ is coefficient of kinetic viscosity, in Pa·s.

Energy equation:

$$\rho c_p\boldsymbol{u}\bullet\nabla t=\nabla\bullet(k\nabla t)+\varphi \tag{13}$$

Where t is temperature in K, k is coefficient of conductivity, in W·(m·K)$^{-1}$; φ is heat source, in W·m^{-3}

Compositional diffusion equation:

$$\boldsymbol{u}\bullet\nabla d=\nabla\bullet(D_{ab}\nabla d)+\varphi_m \tag{14}$$

Where d is humidity, in kg·kg^{-1}; D_{ab} is coefficient of mass transfer, in m^2·s^{-1}; φ_m is humidity source, in kg·m^{-3}.

heat source of flue gas:

$$\varphi_g=2\frac{h_g\left(t_f-t_g\right)}{l_g} \tag{15}$$

Where h means convective heat transfer coefficient, W·(m^2·K)$^{-1}$; l is width of the channel, in m. Subscript f means water films.

heat source of fresh air:

$$\varphi_a=2\frac{h_a\left(t_f-t_a\right)}{l_a}-h_v(t_a)\bullet u\frac{\partial d_a}{\partial y}\rho_a+2\frac{h_m\left(d_g-d_a\right)\rho_a}{l_a}h_v\left(t_f\right) \tag{16}$$

Humidity source:

$$\varphi_m=2\frac{h_m(d_s-d_a)}{l_a} \tag{17}$$

Where $h_v(t_a)$ and $h_v\left(t_f\right)$ means vapor enthalpy in air temperature and water film temperature respectively, in kJ·kg^{-1}; h_m means convective mass transfer coefficient of air and water film, in m·s^{-1}. Subscript a means air; subscript s means saturated air film on the surface of water film.

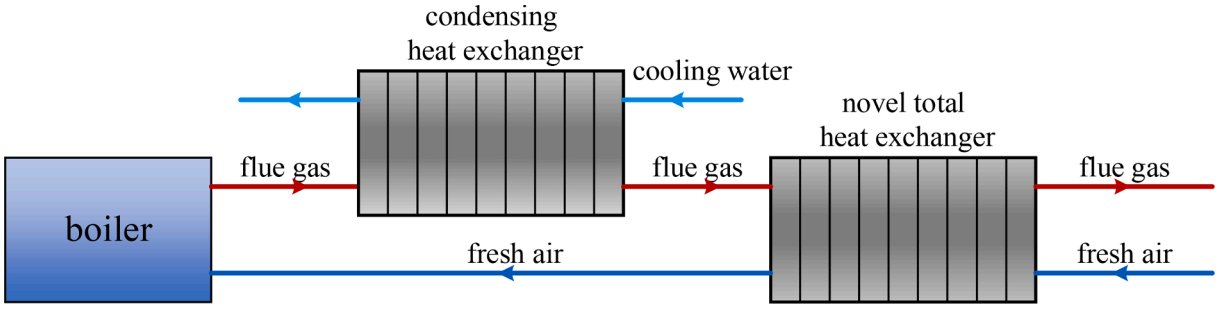

Fig. 7. The scheme of boilers equipped with NTHE.

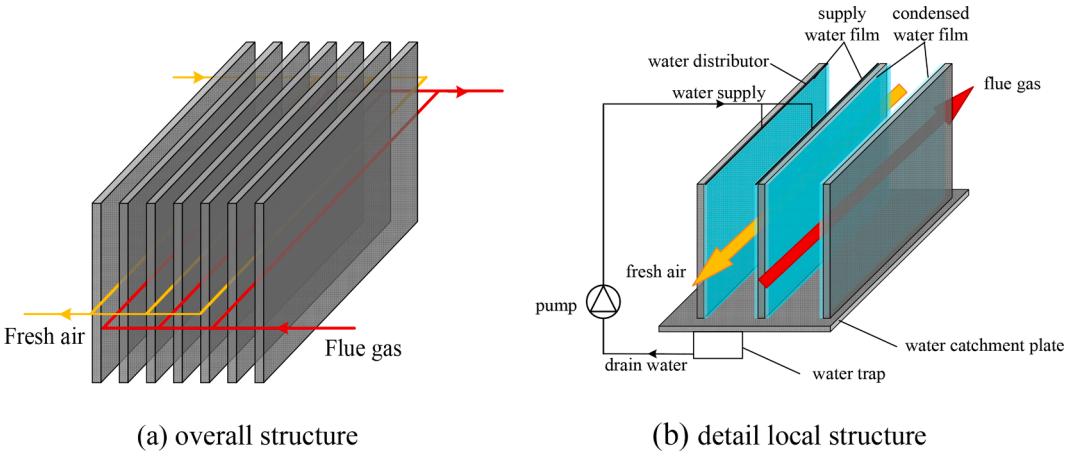

Fig. 8. Structure of the novel total heat exchanger.

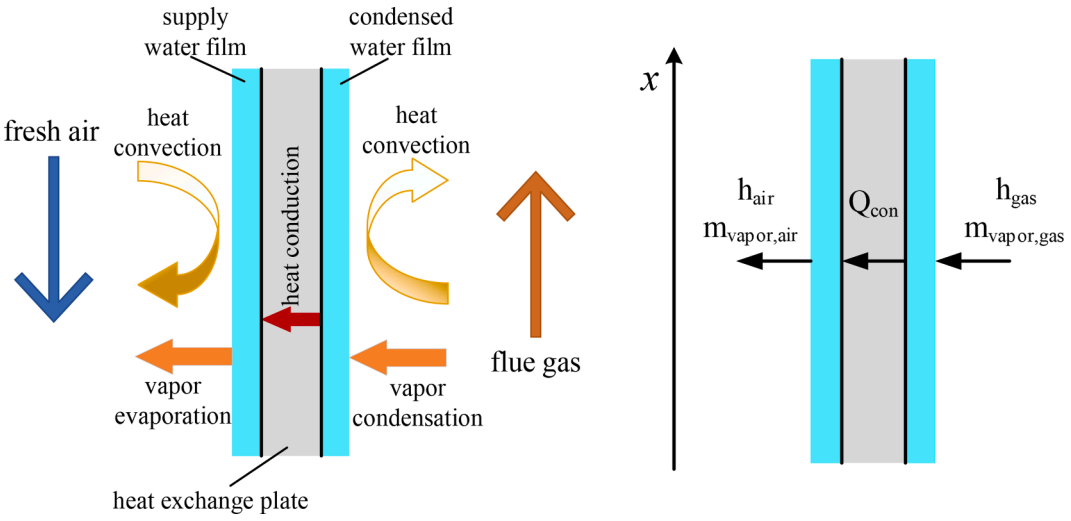

Fig. 9. Heat and mass transfer process of NTHE.

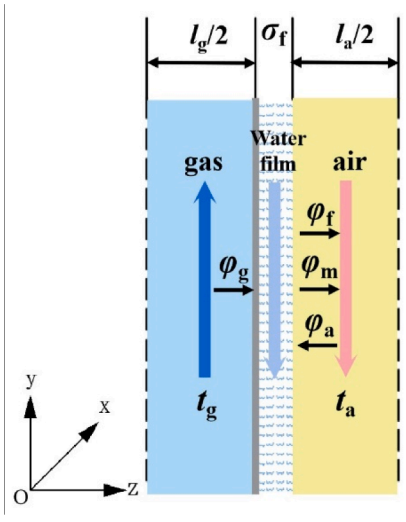

Fig. 10. Physical model of total heat exchanger.

Heat source of water film:

$$\varphi_f = \frac{h_g(t_g - t_f)}{\delta_f} + \frac{h_a(t_a - t_f)}{\delta_f} - r\frac{h_m(d_g - d_a)\rho_a}{\delta_f} \tag{18}$$

Where δ_f is width of water film, in m.

Nu number of dry flue gas is put forward by empirical equation (Özisik, 1985):

$$Nu_{g,d} = 8.235 \tag{19}$$

Nu of saturated flue gas:

$$Nu_{g,s} = Nu_{g,d}\frac{C_{p,g,s}}{C_{p,g,d}} \tag{20}$$

Where $C_{p,g,d}$ means heat capacity of dry flue gas, in kJ·(kg·K)$^{-1}$; $C_{p,g,s}$ means heat capacity of saturated flue gas, in kJ·(kg·K)$^{-1}$.

Both sensible heat transfer and latent heat transfer exists in air channel. Convective heat transfer coefficient of air and water film is estimated by criterion correlation expression for direct evaporative cooling which is put forward by Dowdy and Karabash (1987):

$$Nu = 0.1\left(\frac{l_e}{\delta}\right)^{0.12} Re^{0.8} Pr^{1/3} \tag{21}$$

$$l_e = \frac{V}{A} \tag{22}$$

Where l_e is characteristic length; Re is Reynolds number; Pr is prandtl number; V is wetting medium volume, in m^3; A is area of wet surface, in m^2.

According to Lewis relation, mass transfer coefficient of air and water film in air channel can be calculated:

$$\frac{h_a}{h_m} = \rho_a c_{p,a} Le^{2/3} \tag{23}$$

Where *Le* is Lewis number.

3.4. Boundary condition

3.4.1. Flue gas

Inlet:

$$t_g = t_{g,in},\ u_g = u_{g,in} \tag{24}$$

Outlet:

$$p_g = 0,\ \frac{\partial t_g}{\partial y} = 0 \tag{25}$$

3.4.2. Water film

Inlet:

$$t_f = t_{f,in},\ u_f = u_{f,in} \tag{26}$$

Outlet:

$$p_f = 0,\ \frac{\partial t_f}{\partial y} = 0 \tag{27}$$

3.4.3. Fresh air

Inlet:

$$t_a = t_{a,in},\ d_a = d_{a,in} \tag{28}$$

Outlet:

$$p_a = 0,\ \frac{\partial t_a}{\partial y} = 0,\ \frac{\partial d_a}{\partial y} = 0 \tag{29}$$

Other boundaries are external surface of the channel, and they are regarded as isolation boundary.

3.5. Grid independence test

Parameters of the test model is listed in Table 1. The calculation region used triangular and quadrilateral grids, and grids with 8473, 14,250, 20375, 26,843, and 32,079 elements were selected for grid independence tests. The resulting flue gas outlet temperatures were 14.60 °C, 14.62 °C, 14.64 °C, 14.64 °C, and 14.65 °C, respectively. Considering both the calculation accuracy and the computational iteration time, a grid with 20,375 elements was selected for simulation calculation.

Table 1
Parameters of the test model.

Parameter	Unit	Value
channel height	m	1.2
channel width	m	0.5
channel spacing	mm	6
thickness of heat exchange plate	mm	0.8
flue gas inlet velocity	m/s	2.5
flue gas inlet temperature	°C	60
fresh air inlet velocity	m/s	2.66
fresh air inlet temperature	°C	0
spray water flow rate	kg/h	2.6
spray water inlet temperature	°C	20

3.6. Model validation

Since there are currently no published experimental data on flue gas-air heat transfer using this type of total heat exchanger, and there is only a small difference between the thermal properties of flue gas and air, such as specific heat, with minimal differences in other parameters such as heat transfer coefficients. Therefore, it is feasible to use air-air heat transfer experiments for model validation.

In this study, the experimental data of Riangvilaikul and Kumar (Riangvilaikul and Kumar, 2010) are used for model validation, and the geometric parameters and operating conditions are consistent with the experimental settings. The heat exchanger plate is 1.2 m long and 0.3 m wide, and the channel spacing is 5 mm. The water temperature for spraying is 28 °C, and the water flow rate is 60 $g{\cdot}h^{-1}$. Under different inlet air conditions (velocity, temperature, and humidity), the comparison of the air outlet temperature between the model and the experimental results is shown in Fig. 11, and the error range is within 6 %, indicating that the mathematical model is applicable, and the assumption of uniform water film thickness is appropriate.

4. Simulation results and discussion analysis

4.1. Simulation parameter settings

In this section, the effects of different flue gas velocities, circulating water flow rates, plate aspect ratios, and channel spacings on the performance of the total heat exchanger are studied and analyzed. In the analysis, the ratio of flue gas to air mass flow rate is kept constant, and the flue gas inlet temperature is fixed at 60 °C. Considering waste heat recovery in winter, the air inlet temperature is set to 0 °C. The reference values and ranges of the studied parameters are shown in Table 2 (Wang et al., 2020; Wang et al., 2019; Rydstrand et al., 2004). In the simulation, excess air coefficient is set as 1.1, so that the composition of the flue gas is shown in Table 3.

Based on the composition and properties of flue gas, excess air coefficient increases, flue gas heat capacity increases, and flue gas characteristics are closer to air, which is not beneficial for total heat exchange. Therefore, high excess air coefficient is not suggested.

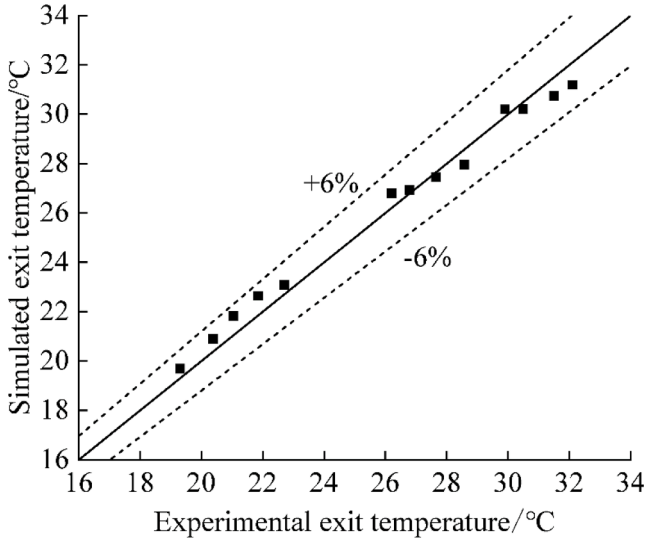

Fig. 11. Relative error between experimental and simulated outlet temperature.

Table 2
The reference value of the research parameter and its range of variation.

Parameter	Symbol	Minimum	Maximum
Flue gas inlet velocity/(m·s^{-1})	$u_{g,in}$	1	5
Mass flow rate of spay water/(kg·h^{-1})	m_f	2	4
length and height ratio of heat exchange plant	C	1	7
Width of channel/(mm)	l	3	10
Area of heat exchange plant/m^2	s	0.6	1

Table 3
Composition of the flue gas.

Composition	N_2	O_2	Ar	CO_2	H_2O
Volume ratio	0.713	0.0174	0.00852	0.0897	0.171

4.2. Performance evaluation

In this analysis, heat transfer efficiency of the total heat exchanger is represented by the total heat transfer efficiency η.

$$\eta = \frac{H_{gas,in} - H_{gas,out}}{H_{gas,in} - H_{gas,0^\circ C}} \tag{30}$$

Where $H_{gas,in}$ means enthalpy of inlet flue gas; $H_{gas,out}$ means enthalpy of outlet flue gas; $H_{gas,0^\circ C}$ means enthalpy of saturated flue gas in 0 °C. In the analysis, we define the enthalpy of saturated flue gas in 0 °C is 0, therefore η can be written as

$$\eta = 1 - \frac{H_{gas,out}}{H_{gas,in}} \tag{31}$$

The amount of heat transfer Q can be written as

$$Q = \Delta h_a \cdot m_a \tag{32}$$

Where Q means the amount of heat transfer, in kW; Δh_a means enthalpy difference of outlet and inlet fresh air, in kJ·kg^{-1} ; m_a means inlet air mass flow, kg·s^{-1}.

4.3. Effects of flue gas inlet velocity

When the ratio of air to spray water mass flow rate is 5.5, the plate aspect ratio is 2.4, and the channel spacing is 6 mm, and the heat exchange area of the plate is 0.6 m^2, 0.8 m^2, and 1 m^2, respectively, the performance of the total heat exchanger varies with the flue gas inlet velocity, as shown in Figs. 12 and 13.

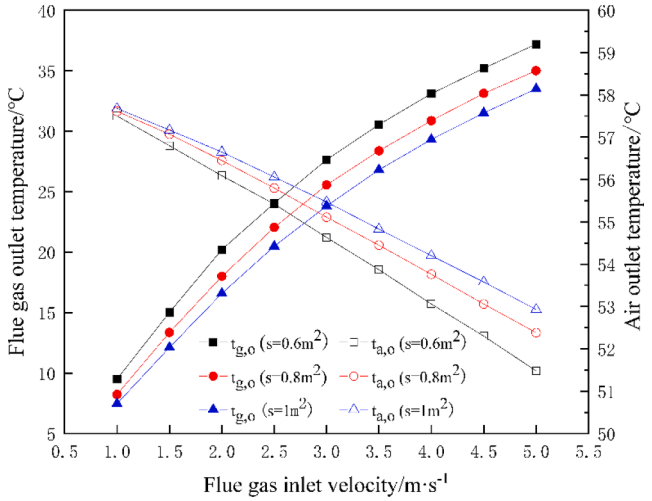

Fig. 12. Effect of flue gas inlet flow rate on flue gas and air outlet temperature.

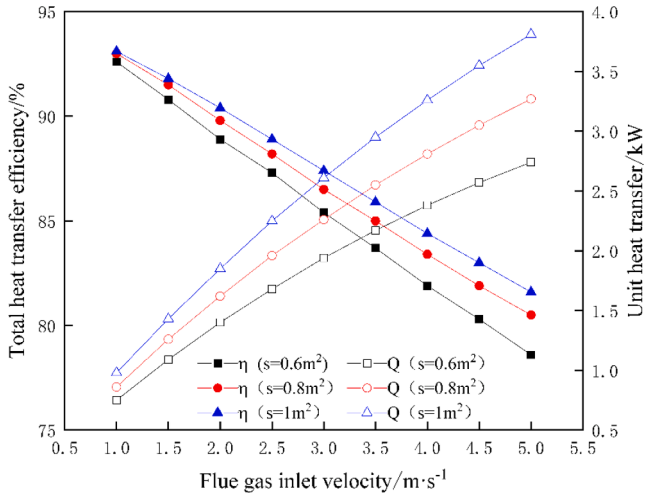

Fig. 13. Effect of flue gas inlet velocity on total heat transfer efficiency and unit heat transfer.

As shown in Figs. 12 and 13, with the increase of flue gas inlet velocity, the flue gas outlet temperature gradually increases, the total heat transfer efficiency decreases, and the unit heat transfer rate increases but the increase rate gradually decreases. For example, when the heat exchange area is 0.6 m^2 and the flue gas inlet velocity increases from 2 m·s^{-1} to 5 m·s^{-1}, the inlet flow rate increases by 2.5 times, but the unit heat transfer rate only increases from 1.4 kW to 2.74 kW, an increase of only 1.96 times.

The effect of flue gas inlet velocity on the total heat transfer efficiency is mainly linear, as the contact time between the flue gas and the heat exchange plate decreases with the increase of flue gas inlet velocity. The flue gas flows out of the channel before fully exchanging heat with the heat exchange plate, causing a decrease in the unit heat transfer rate and an increase in the average outlet temperature, resulting in a decrease in the total heat transfer efficiency.

4.4. Effects of spray water mass flow rate

When the flue gas inlet velocity is 2.5 m·s^{-1}, the plate aspect ratio is 2.4, and the channel spacing is 6 mm, and the heat exchange area of the plate is 0.6 m^2, 0.8 m^2, and 1 m^2, respectively, the performance of the total heat exchanger varies with the spray water mass flow rate, as shown in Figs. 14 and 15.

According to Figs. 14 and 15, the spray water flow rate has little

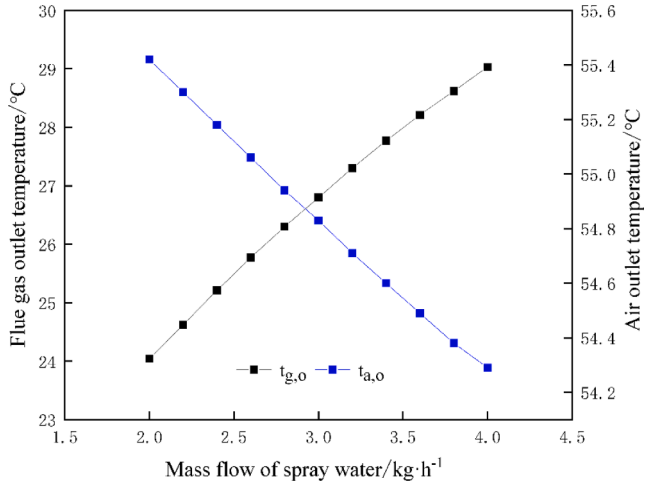

Fig. 14. Effect of spray water flow rate on flue gas and air outlet temperature.

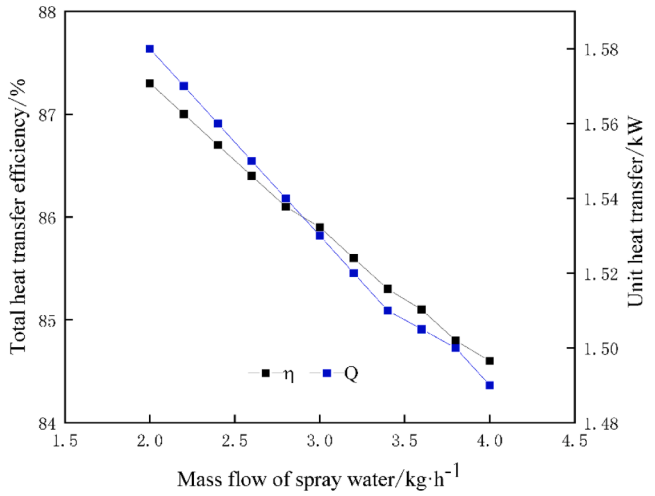

Fig. 15. Effect of spray water flow rate on total heat transfer efficiency and unit heat transfer.

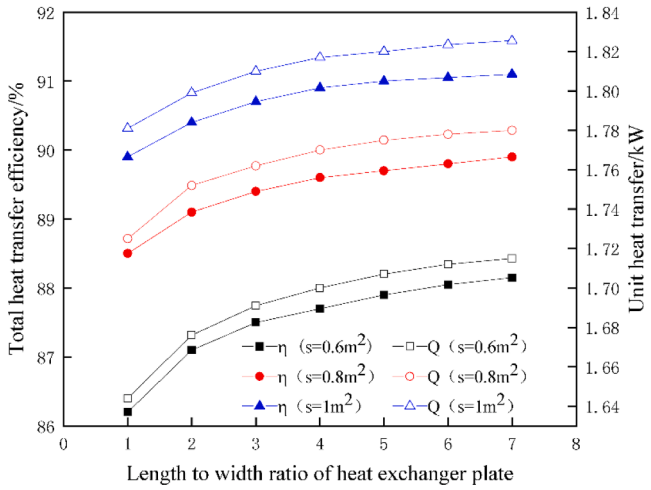

Fig. 17. Effect of length–width ratio on total heat transfer efficiency and unit heat transfer.

effect on the overall heat transfer efficiency compared to other factors. As the mass flow rate of spray water increases, the flue gas outlet temperature rises, and both the overall heat transfer efficiency and the unit heat transfer decrease. The main reason why the mass flow rate of circulating water affects the heat transfer efficiency of the heat exchanger is that the convective heat transfer coefficient on the water film surface decreases with an increase in the mass flow rate of spray water. Additionally, as the mass flow rate of spray water increases, the overall water film temperature in the channel decreases, resulting in a decrease in the moisture content of the saturated air on the water film surface. This leads to a reduction in the transfer rate of the water film to the air, resulting in a decrease in the overall heat transfer rate and the overall heat transfer efficiency.

Therefore, it is better to have a smaller mass flow rate of spray water if it meets the requirement of providing enough water to maintain a saturated state. Furthermore, after changing other parameters such as flue gas velocity and channel spacing, it is found that the ratio of air to mass flow rate of spray water has a consistent influence on the heat exchanger performance regardless of other factors.

4.5. The Effect of heat transfer plate length-to-width ratio

When the flue gas volumetric flow rate is 3.75×10^{-3} m^3/s, the ratio of air to mass flow rate of spray water is 5.5, and the channel spacing is 6 mm, the heat transfer performance of the heat exchanger varies with the aspect ratio of the heat transfer plate when the heat transfer plate area is 0.6 m^2, 0.8 m^2, and 1 m^2, as shown in Figs. 16 and 17.

According to Figs. 16 and 17, as the aspect ratio of the heat transfer plate increases, the flue gas outlet temperature decreases, and the overall heat transfer efficiency first rapidly increases and then tends to stabilize. To achieve higher heat transfer efficiency and heat transfer, it is recommended to use an aspect ratio of 3 or higher.

The reason why the aspect ratio of the heat transfer plate affects the heat transfer efficiency of the heat exchanger is that when the heat transfer plate area is constant, as the aspect ratio increases, the cross-sectional area of the flue gas inlet decreases. Since the inlet flow rate of the flue gas remains constant, the inlet velocity of the flue gas increases, and the ratio of the inlet velocity to the plate length remains the same. The flue gas heat transfer time remains constant, but the increase in flue gas velocity increases the heat and mass transfer coefficients, thereby increasing the overall heat transfer efficiency.

4.6. Effects of channel spacing on heat transfer performance of heat exchanger

When the inlet velocity of flue gas is 2.5 m/s, the ratio of air to spray water mass flow rate is 5.5, and the length–width ratio of heat transfer plate is 2.4, the heat transfer area of the heat exchanger is 0.6 m^2, 0.8 m^2

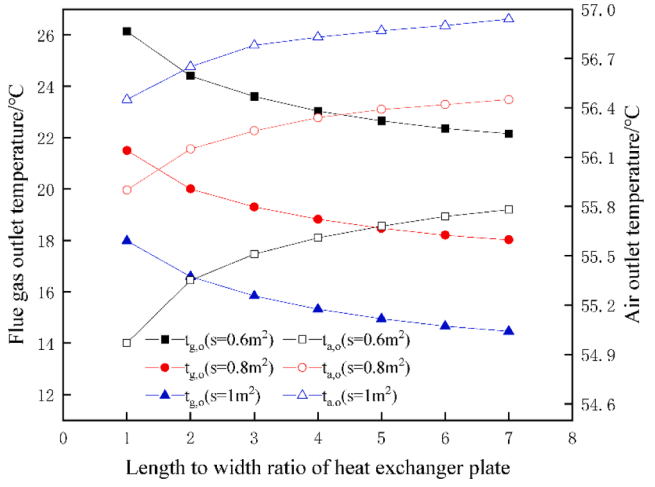

Fig. 16. Effect of length to width ratio on flue gas and air outlet temperature.

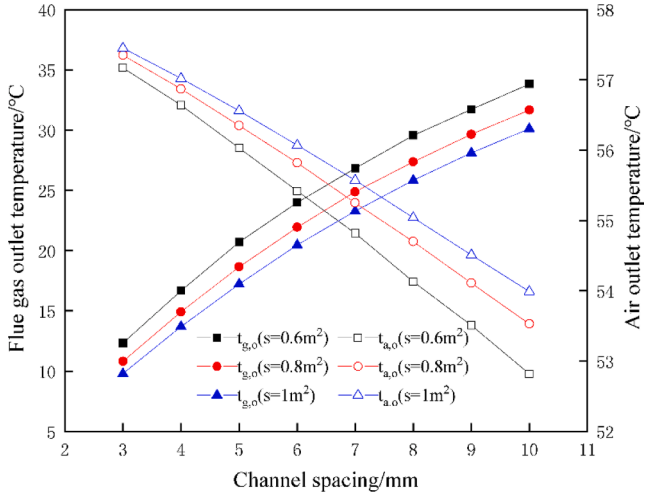

Fig. 18. Effect of passage spacing on flue gas and air outlet temperature.

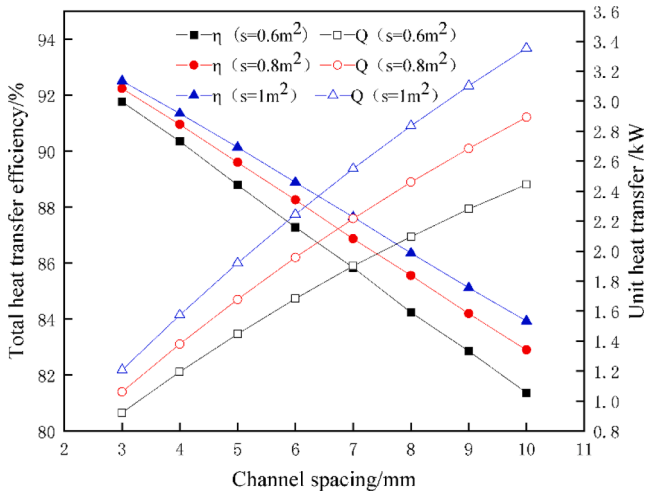

Fig. 19. Influence of channel spacing on total heat transfer efficiency and unit heat transfer.

and 1 m^2, respectively. The performance of the total heat exchanger varies with the channel spacing as shown in Figs. 18 and 19.

Figs. 18 and 19 show that with the increase of channel spacing, the overall heat transfer efficiency decreases linearly, while the unit heat transfer rate increases but the growth trend gradually slows down. When the heat transfer area is 0.6 m^2 and the channel spacing increases from 3 mm to 10 mm, the unit heat transfer rate increases from 1.45 kW to 2.45 kW, with a growth rate of 69 %.

The main reason for the effect of channel spacing on the heat transfer performance of the heat exchanger is that as the channel spacing increases, the mass flow rates of flue gas and air increase simultaneously, leading to an increase in heat transfer rate. However, because the fluid at the center of the channel is far from the heat transfer plate and is discharged before being fully heat exchanged, the heat transfer efficiency decreases.

5. Total heat exchange efficiency comparison

At present, deep waste heat recovery technologies without extra heat or electricity power mainly are BEVP system and EW system. In this part, NTHE is compared to DT subsystem and EW system.

5.1. Comparing to DT subsystem

To promote performance of BEVP system, DT subsystem can be divided into several stages (see Fig. 20). In this part, limit performance of BEVP system with 1, 2, 3 and 4 stages are compared to NTHE system.

According to the result get by Wang et al. (2020), total heat transfer process of NTHE system corresponding to the limit performance of DT system with 1, 2, 3 and 4 stages is shown in Fig. 21, and the limit heat transfer efficiency of DT system with 1, 2, 3 and 4 stages are 83 %, 93 %, 96 % and 98 %. According to the result above, under limit conditions, flue gas temperature can be cooled down to 0 °C using NTHE system. Therefore, the limit heat transfer efficiency of NTHE system is 100 %.

Furthermore, take heat transfer temperature difference into consider, heat transfer efficiency of DT system is going down. In the article, temperature difference of spray tower is 1.5 °C, flue gas outlet

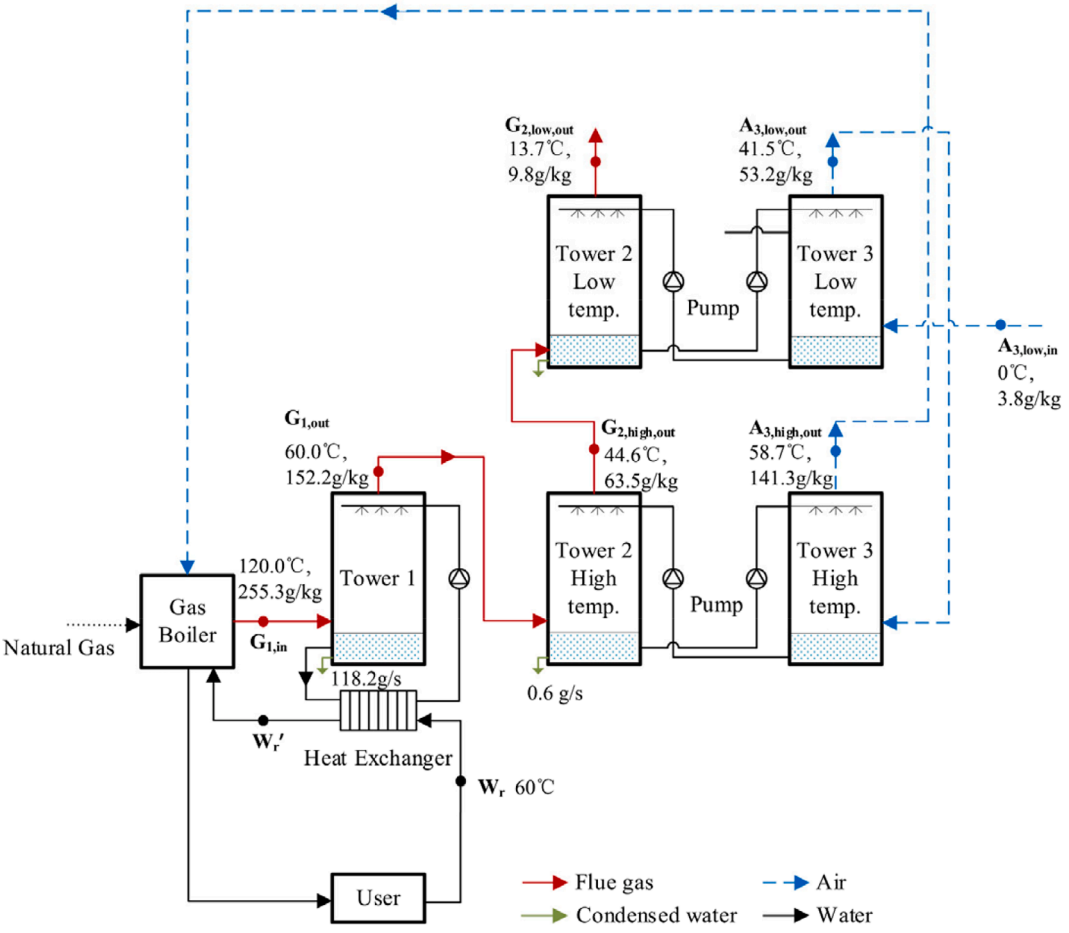

Fig. 20. The scheme of DT subsystem with sever segments (two segments as an example) (Wang et al., 2020).

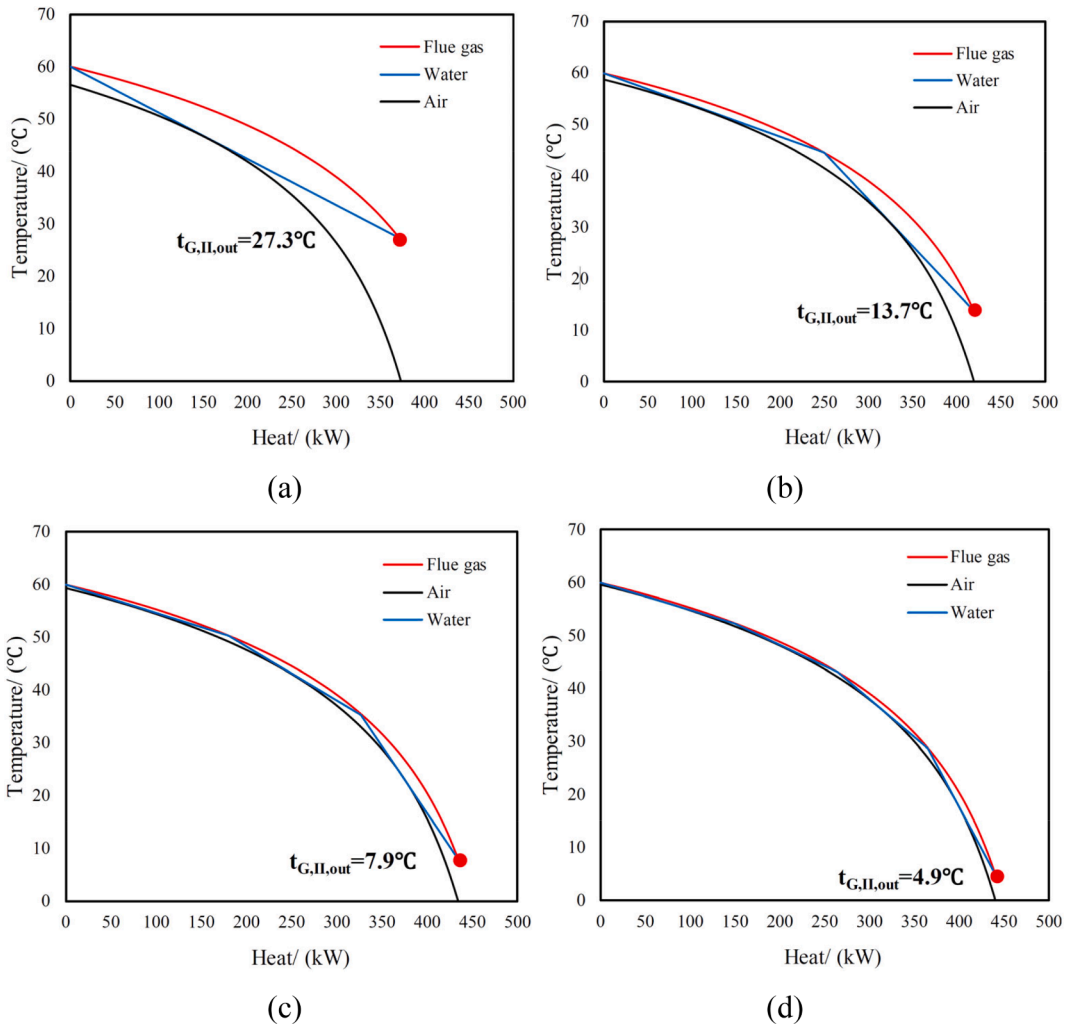

Fig. 21. Process corresponding to BEVP system (Wang et al., 2020): (a) 1 segment; (b) 2 segments; (c) 3 segments; (d) 4 segments.

temperature of DT system with 1, 2, 3 and 4 stages rise to 34.2 °C, 26.2 °C, 23.0 °C, 21.4 °C, respectively. Correspondingly, heat transfer efficiency of DT system with 1, 2, 3 and 4 stages drop down to 74 %, 84 %, 87 % and 88 %, respectively. According to the result, the efficient of the novel total heat exchanger and 3-stage DT system are about the same. However, the 3-stage DT systems have high operational requirements, so that it is difficult to achieve the theoretical efficiency in practice.

Therefore, NTHE system can reach limit performance of BEVP system with 2 stages (Wang et al., 2020). Further, when temperature difference of spray tower is taken into consider, heat transfer efficiency of NTHE system can 7 % higher than 2-segment BEVP system.

5.2. Comparing to EW subsystem

According to the result get by Men et al. (2019), under the following conditions: fresh air temperature $T_{air} = 10$ °C; inlet flue gas temperature $T_{gas} = 45$ °C; Rotary speed of EW rpm > 8, efficiency of EW is 79–84 %.

According to the analyzed above, total heat transfer efficiency of NTHE system is around 87 %. It is 5 % higher than EW system. Further, when we adjust the parameters, total heat transfer efficiency of NTHE system can reach 91.8 %, which is 10 % higher than EW system.

6. Conclusion

In this paper, a countercurrent evaporation–condensation type full heat exchanger suitable for flue gas waste heat recovery is proposed. The feasibility of achieving air-flue gas full heat exchange is demonstrated through mathematical derivation. Secondly, a two-dimensional model describing the heat and mass transfer process is established, and based on the simulation, the influence of four parameters, namely flue gas inlet velocity, spray water mass flow rate, heat exchanger length-to-width ratio, and channel spacing on the heat transfer performance of the full heat exchanger is studied. The following conclusions are drawn:

1. If the difference in thermal properties between flue gas and air is ignored, the heat transfer efficiency of the full heat exchanger can reach 100 % in the limit case of infinitely large heat transfer plate area.
2. With the increase of flue gas inlet velocity, the heat transfer efficiency of the heat exchanger decreases, and the unit heat transfer increases but the growth rate gradually decreases. The unit heat transfer and heat transfer efficiency both decrease with the increase of spray water flow rate. Therefore, under the condition of meeting the water quantity required to maintain air saturation, the smaller the spray water flow rate, the better the performance of the heat exchanger.
3. When the heat transfer plate area is constant, the larger the length-to-width ratio, the higher the full heat transfer efficiency and unit heat transfer. Therefore, it is recommended to choose a length-to-width ratio above 3. With the increase of channel spacing, the heat transfer efficiency decreases and the unit heat transfer increases.

4. According to the simulation results, the total heat transfer efficiency is about 78 % to 92 %. Comparing to DT subsystem, NTHE system can reach limit performance of BEVP system with 2 stages and when temperature difference of spray tower is taken into consider, heat transfer efficiency of NTHE system can 7 % higher than 2-segment BEVP system. Comparing to EW subsystem, total heat transfer efficiency of NTHE system is 10 % higher than EW system.

CRediT authorship contribution statement

Jing Hua: Conceptualization, Investigation, Methodology, Software, Writing – original draft. **Jingyi Wang:** Conceptualization, Writing – review & editing. **Tingting Zhu:** Conceptualization, Validation, Writing – review & editing.

Declaration of competing interest

The authors declare that they have no known competing financial interests or personal relationships that could have appeared to influence the work reported in this paper.

Data availability

Data will be made available on request.

Acknowledgement

The authors acknowledge the support from Shenzhen Finance Bureau (HA11409053), and from Department of Education of Guangdong Province (2021KQNCX271). The authors also gratefully acknowledge the financial support provided by the National Natural Science Foundation Programs of China (Grant No. 51906177).

References

Cui, Z., Qian, D.u., Gao, J., Bie, R., Li, D., 2020. Development of a direct contact heat exchanger for energy and water recovery from humid flue gas. Appl. Therm. Eng. 173, 115214.

Dowdy, J.A., Karabash, N.S. 1987. Experimental determination of heat and mass transfer coefficients in rigid impregnated cellulose evaporative media.

El-Shafie, M., Khalil Bassiouny, M., Kambara, S., El-Behery, S.M., Hussien, A.A., 2021. Design of a heat recovery unit using exhaust gases for energy savings in an absorption air conditioning unit. Appl. Therm. Eng. 194, 117031.

Han, Z.X., Guo, J., Zhang, H., Chen, J., Huai, X., Cui, X., 2021. Experimental and numerical studies on novel airfoil fins heat exchanger in flue gas heat recovery system. Appl. Therm. Eng. 192, 116939.

Jiang, Y., Zhang, H., Wang, Y., You, S., Zhangxiang, W.u., Song, Z., 2021. Performance investigation of a counterflow packing tower for flue gas waste heat recovery. Appl. Therm. Eng. 196, 117315.

Ma, H., Liang, N., Zhang, N.a., Luo, X., Hou, C., Wang, G., 2021. Simulation of a novel waste heat recovery system with sulfide-containing flue gas. Appl. Therm. Eng. 187, 116556.

Men, Y., Liu, X., Zhang, T., Xi, X.u., Jiang, Y.i., 2019. Novel flue gas waste heat recovery system equipped with enthalpy wheel. Energ. Conver. Manage. 196, 649–663.

Men, Y., Liu, X., Zhang, T., 2021. Performance comparison of different total heat exchangers applied for waste heat recovery. Appl. Therm. Eng. 182, 115715.

Men, Y., Liu, X., Zhang, T., 2022. Performance research and application of the vapor pump boiler equipped with flue gas recirculation system. Energ. Conver. Manage. 254, 115201.

Min, C., Yang, X., He, J., Wang, K., Xie, L., Onwude, D.I., Zhang, W., Wu, H., 2021. Experimental investigation on heat recovery from flue gas using falling film method. Therm. Sci. Eng. Progr. 22, 100839.

Mohammadaliha, N., Amani, M., Bahrami, M., 2022. A Thermal-hydraulic assessment of condensing tube bank heat exchangers for heat and water recovery from flue gas. Appl. Therm. Eng. 215, 118976.

Özisik, M.N., 1985. Heat Transfer: A Basic Approach. McGraw-Hill College, New York.

Riangvilaikul, B., Kumar, S., 2010. An experimental study of a novel dew point evaporative cooling system. Energy Build. 42 (5), 637–644.

Rydstrand, M.C., Westermark, M.O., Bartlett, M.A., 2004. An analysis of the efficiency and economy of humidified gas turbines in district heating applications. Energy 29 (12/15), 1945–1961.

Wang, J., Hua, J., Lin, F., Wang, Z., Zhang, S., 2019. A theoretical fundamental investigation on boilers equipped with vapor-pump system for Flue-Gas Heat and Moisture Recovery. Energy 171, 956–970.

Wang, J., Hua, J., Lin, F., Zhou, D., 2020. Effect of gas nonlinearity on boilers equipped with vapor-pump (BEVP) system for flue-gas heat and moisture recovery. Energy 198, 117375.

Wang, X., Zhuo, J., Liu, J., Li, S., 2020. Synergetic process of condensing heat exchanger and absorption heat pump for waste heat and water recovery from flue gas. Appl. Energy 261, 114401.

Wei, H., Huang, S., Zhang, X., 2022. Experimental and simulation study on heat and mass transfer characteristics in direct-contact total heat exchanger for flue gas heat recovery. Appl. Therm. Eng. 200, 117657.

Xiao, L., Yang, M., Zhao, S., Yuan, W.-Z., Huang, S.-M., 2019. Entropy generation analysis of heat and water recovery from flue gas by transport membrane condenser. Energy 174, 835–847.

Xiao, L., Yang, M., Yuan, W.-Z., Huang, S.-M., 2021. Macroporous ceramic membrane condenser for water and heat recovery from flue gas. Appl. Therm. Eng. 186, 116512.

Yang, B., Yuan, W., Lin, F., Zhang, S., Wei, M., Guo, D., 2020. Techno-economic study of full-open absorption heat pump applied to flue gas total heat recovery. Energy 190, 116429.

Yang, B.o., Yuan, W., 2022. Performance analysis of a novel two-stage membrane waste heat recovery system. Appl. Therm. Eng. 215, 118952.

Yu, J., Zhao, R., Zhao, M., Wu, Z., Zhang, P., Zhang, Y., Ma, H., 2021. Comparative analysis of working fluids for heat pump-type flue-gas cooling–reheating system. Appl. Therm. Eng. 193, 117019.

Zhang, H., Dong, Y., Lai, Y., Zhang, H., Zhang, X., 2021. Waste heat recovery from coal-fired boiler flue gas: Performance optimization of a new open absorption heat pump. Appl. Therm. Eng. 183, 116111.

Zhang, H., Lai, Y., Yang, X., Li, C., Dong, Y., 2022. Non-evaporative solvent extraction technology applied to water and heat recovery from low-temperature flue gas: Parametric analysis and feasibility evaluation. Energy 244, 123062.

Zhang, Q., Niu, Y., Niu, X.Y., Sun, D., Xiao, X., Shen, Q., Wang, G., 2020. Experimental study of flue gas condensing heat recovery synergized with low NOx emission system. Appl. Energy 269, 115091.

Zhang, C., Yang, Y., Fan, L., Huang, X., 2020. Numerical study on operating characteristics of self-driven total heat recovery system for wet-hot flue gas. Appl. Therm. Eng. 173, 115223.